Marine Geology 345 (2013) 314–326

Contents lists available at ScienceDirect

Marine Geology

journal homepage: www.elsevier.com/locate/margeo

Seasonal variations in suspended-sediment dynamics in the tidal reach of an estuarine tributary

Maureen A. Downing-Kunz *, David H. Schoellhamer

U.S. Geological Survey, Placer Hall, 6000 J Street, Sacramento, CA 95819, USA

ARTICLE INFO

Article history:
Received 6 April 2012
Received in revised form 25 March 2013
Accepted 27 March 2013
Available online 18 April 2013

Keywords:
sediment transport
suspended sediment
sediment flux
estuarine tributary
San Francisco Bay
seasonal variation

ABSTRACT

Quantifying sediment supply from estuarine tributaries is an important component of developing a sediment budget, and common techniques for estimating supply are based on gages located above tidal influence. However, tidal interactions near tributary mouths can affect the magnitude and direction of sediment supply to the open waters of the estuary. We investigated suspended-sediment dynamics in the tidal reach of Corte Madera Creek, an estuarine tributary of San Francisco Bay, using moored acoustic and optical instruments. Flux of both water and suspended-sediment were calculated from observed water velocity and turbidity for two periods in each of wet and dry seasons during 2010. During wet periods, net suspended-sediment flux was seaward; tidally filtered flux was dominated by the advective component. In contrast, during dry periods, net flux was landward; tidally filtered flux was dominated by the dispersive component. The mechanisms generating this landward flux varied; during summer we attributed wind–wave resuspension in the estuary and subsequent transport on flood tides, whereas during autumn we attributed increased spring tide flood velocity magnitude leading to local resuspension. A quadrant analysis similar to that employed in turbulence studies was developed to summarize flux time series by quantifying the relative importance of sediment transport events. These events are categorized by the direction of velocity (flood vs. ebb) and the magnitude of concentration relative to tidally averaged conditions (relatively turbid vs. relatively clear). During wet periods, suspended-sediment flux was greatest in magnitude during relatively turbid ebbs, whereas during dry periods it was greatest in magnitude during relatively turbid floods. A conceptual model was developed to generalize seasonal differences in suspended-sediment dynamics; model application to this study demonstrated the importance of few, relatively large events on net suspended-sediment flux. These results suggest that other estuarine tributaries may alternate seasonally as sediment sinks or sources, leading to the conclusion that calculations of estuary sediment supply from local tributaries that do not account for tidal reaches may be overestimates.

Published by Elsevier B.V.

1. Introduction

Sediment is supplied to San Francisco Bay by discharge from rivers and creeks, and by exchange with the Pacific Ocean. Recent studies have shown that the sediment supply to San Francisco Bay from the Sacramento–San Joaquin Delta has been steadily decreasing over time (e.g., Porterfield, 1980; Wright and Schoellhamer, 2004). This is due in part to diminishment of a pulse of sediment from hydraulic mining in the watershed, damming of upstream tributaries, deposition in flood bypasses, and river bank protection. Given this trend, the local watersheds of San Francisco Bay are increasingly important in supplying sediment to the estuary. These local watersheds are drained by tidal creeks that enter the Bay seaward of Mallard Island (near the confluence of Sacramento River and San Joaquin River). While providing only 10% of the freshwater influx to San Francisco Bay, these local tributaries are estimated to presently supply approximately 60% of the sediment influx (McKee et al., in 2013–this issue).

In San Francisco Bay, existing studies of sediment supply to open waters of the estuary from local tributaries rely on measurements made above tidal influence and thus do not account for the tidal reach (e.g., Porterfield, 1980; Lewicki and McKee, 2009). These studies have demonstrated great seasonal variability in sediment supply. Most sediment supplied from these local tributaries is episodic; studies estimate that 50% of the annual discharge and nearly 90% of the sediment load occur during a few days per year (Kroll, 1975; Warrick and Milliman, 2003; McKee et al., 2003; Lewicki and McKee, 2009). Given this seasonal variability, these local tributaries can be thought of as intermittent streams, connected to the estuary by a tidal reach. During rain events, watershed runoff occurs and the tributaries act like rivers, conveying flow and sediment from the watershed. However, this conveyance and the resulting suspended-sediment flux are affected by the timing and size of the watershed flood pulse relative to those of the tidal

* Corresponding author. Tel.: +1 916 278 3051.
E-mail address: mokunz@usgs.gov (M.A. Downing-Kunz).

0025-3227/$ – see front matter. Published by Elsevier B.V.
http://dx.doi.org/10.1016/j.margeo.2013.03.005

cycle. During dry periods, watershed runoff is low to nonexistent, and the tidal reaches of these tributaries act as an extension of the estuary. During these periods, the direction of net suspended-sediment flux is not known, and these tidal reaches may act as sediment sinks, as has been shown for larger estuarine tributaries (e.g., Schubel and Carter, 1976; Geyer et al., 2001).

The effect of the tidal reaches of local tributaries on suspended-sediment supply to an estuary is less studied. Understanding this effect is important to regional management of the sediment system, including flood control, navigation, habitat restoration, and shoreline protection. The purpose of this study is to examine differences in sediment transport between wet and dry seasons in the tidal reach of a San Francisco Bay tributary, Corte Madera Creek (Fig. 1). The local tributaries of San Francisco Bay share similar hydrology (Lewicki and McKee, 2009), thus the general sediment transport characteristics in the tidal reach of Corte Madera Creek are expected to be similar in the other tributaries.

2. Study site

The study site is located 15 km north of San Francisco, California, at the mouth of Corte Madera Creek (Fig. 1). The Corte Madera Creek watershed drains 73 km^2 located in Marin County, California. The tidally affected reach of Corte Madera Creek is approximately 5.5 km long and drains into Corte Madera Bay, an embayment of San Francisco Bay. The tidal reach is bordered by a highly urbanized area and the flow is generally constrained to the channel, though adjacent marsh is present at a few locations totaling about 0.1 km^2. Near the mouth of the creek are a ferry terminal (operating year round) and a dredged navigation channel with water depth of approximately 4 m relative to mean lower low water (MLLW). The tidal reach experiences a semidiurnal tide with a mean range of 1.3 m near the creek mouth (based on NOAA tide predictions for Station 9414874, http://tidesandcurrents.noaa.gov/tide_predictions.shtml). Most annual precipitation (124 cm yr^{-1}) occurs as rain in the six months between October 1 and April 1 (Lewicki and McKee, 2009).

3. Materials and methods

Water velocity and discharge, suspended-sediment concentration, water temperature, and salinity were measured at a site 0.8 km upstream of the mouth of Corte Madera Creek, referred to as the "Mouth" station. Instrumentation was attached to an abandoned railroad bridge pier; the channel width at this location is approximately 100 m.

3.1. Discharge

Discharge (Q) at the Mouth was determined using the index velocity method (Ruhl and Simpson, 2005). In this method, two calibrations are required: first, stage (S) measured at the study site is calibrated to cross-sectional area (A) of the channel. Second, index velocity (V_i) measured at the study site is calibrated to mean channel velocity (V_a) measured from boat-mounted instrumentation and the stage–area relation.

Along-channel velocity measured by a two-beam, side-looking acoustic Doppler velocity meter (ADVM, EasyQ 2 MHz, NortekUSA, Boston, MA; the use of firm, trade, and brand names is for identification purposes only and does not constitute endorsement by the USGS) was used as the

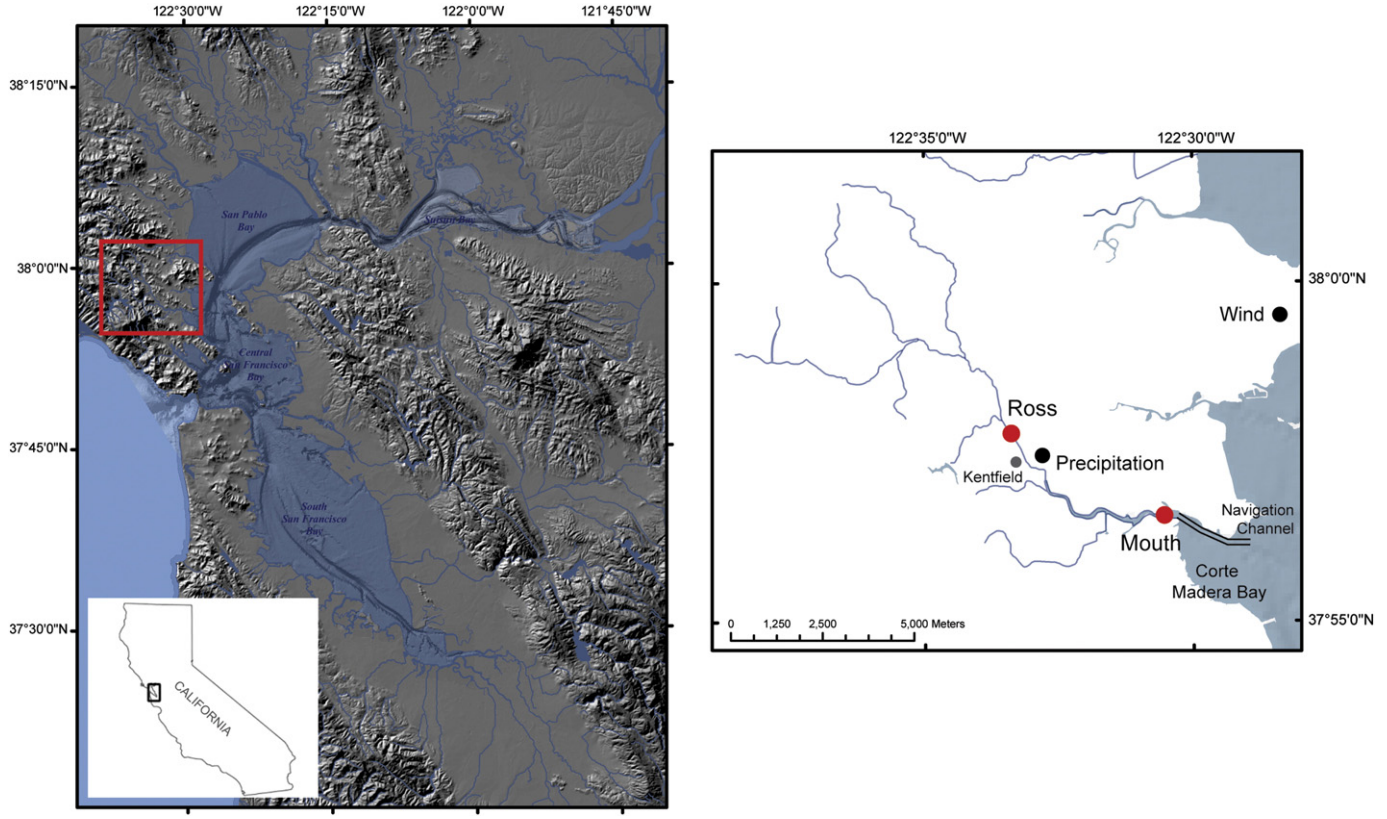

Fig. 1. Left — Overview map of San Francisco Bay with study area delineated by box. Right — Map of Corte Madera Creek watershed with locations of monitoring stations: upstream of tidal influence ('Ross', USGS site 11460000) and at tributary mouth ('Mouth', USGS site 11460090). Wind velocity data were obtained from the Point San Pedro meteorological station ('Wind', site 157, operated by CA Dept. of Water Resources). Precipitation data were obtained from the Kentfield station ('Precipitation', site 5261, operated by Marin County Flood Control and Water Conservation District). Dredged navigation channel outlined by dark solid lines in Corte Madera Bay.

gage for index velocity (V_i). The ADVM was mounted 0.91 m above the bed, with the two orthogonal velocity beams pointing toward the center of the channel. The ADVM records velocity in three bins in the horizontal x- and y-plane as a 4-min mean every 15 min. The coordinate system of the ADVM was rotated onto the primary flow direction by determining the angle of maximum variance. This rotation yields along- and across-channel velocities; V_i was selected as the along-channel velocity in a 1 m cell centered approximately 3 m from the instrument. This sampling volume was located near the centerline of the channel, approximately 40 m from the right bank. The ADVM also measures stage (S) via a vertical beam that reflects off the water surface; stage is recorded as a 2-min mean every 15 min.

Instantaneous measurements of channel discharge were collected at a transect located 80 m downstream of the Mouth station using a boat-mounted, downward-looking acoustic Doppler current profiler (ADCP, Workhorse 1.2 MHz, RD Instruments, San Diego, CA). Repeated transects across the channel were performed to obtain measurements for various phases of the tidal cycle; most measurements were made during strong spring tides to capture the greatest tidal velocities. Instantaneous channel area was estimated using the geometry of the cross section obtained from a discharge transect collected near high tide using a hydroboard-mounted ADCP towed across the channel via kayak. The kayak allowed a survey of the entire cross section. The stage vs. channel area relationship was calculated using the USGS software AreaComp2 ver. 1.04 (http://hydroacoustics.usgs.gov/index.shtml). A quadratic polynomial was fit to this stage–area relation to develop the continuous time series of A.

Instantaneous discharge from the ADCP was divided by channel area (computed from stage–area relation at time of transect) to yield instantaneous V_a. The continuous time series of V_a was developed by linear regression of instantaneous V_i (linearly interpolated to transect times) and instantaneous V_a. Finally, the continuous time series of discharge (Q) is calculated as the product of V_a and A. In this study, positive Q denotes ebb tide and negative Q denotes flood tide.

3.2. Suspended-sediment concentration and flux

Suspended-sediment concentrations (SSC) near the mouth of Corte Madera Creek were determined by calibrating turbidity sensor output to SSC in water samples collected in situ. A multiparameter water quality sonde (Model 6920 V2, YSI, Inc., Yellow Springs, OH) equipped with an optical turbidity sensor (Model 6136, YSI, Inc., Yellow Springs, OH) was mounted 1.31 m above the bed at the Mouth station and recorded instantaneous values every 15 min. This optical sensor is self-cleaning and measures the intensity of light scattered at 90° between a light-emitting diode and a photodiode detector; output is in formazin nephelometric units (FNU). Turbidity sensors are sensitive to biological fouling; the instrument was recovered for cleaning and calibration checks every 3–8 weeks. Fouling was greatest during the summer. Calibration of turbidity to SSC was performed by collecting water samples during site visits. Water samples were collected using a boat-mounted isokinetic sampler (Model D-74, Edwards and Glysson, 1999) at the same cross section as for discharge measurements (described above). The equal-discharge-increment method was employed to approximate average conditions in the channel (Edwards and Glysson, 1999). Using measurements of channel discharge and geometry from the ADCP transects, the cross section was divided into five areas of equal discharge. Velocity-weighted depth-integrated samples were collected at the centroids of these five areas and analyzed to quantify SSC. The mean value of these five SSC samples was taken as the channel-average SSC; the corresponding sampling time was taken as the midpoint of elapsed time for all five samples. Turbidity at the time of SSC sampling (linearly interpolated as needed) was related to channel-average SSC by linear regression using the robust, nonparametric repeated median method (Siegel, 1982). This method yields a calibration curve that was applied to the turbidity record to obtain the continuous time series of channel-average SSC (denoted as C). The time series of instantaneous suspended-sediment flux (Q_s) at the Mouth station was calculated as the product of channel discharge (Q) and channel-average SSC (C).

3.3. Ancillary data

Additional data were utilized to support the analysis, including wind velocity, precipitation, watershed discharge, and watershed suspended-sediment flux. Time series of wind velocity (magnitude and direction) was obtained from the Point San Pedro meteorological station (Site 157, operated by California Department of Water Resources, California Irrigation Management Information System; http://www.cimis.water.ca.gov/). Time series of precipitation measured at Kentfield, CA (Site 5261) was obtained from Marin County Flood Control and Water Conservation District (http://marin.onerain.com/). Watershed input of flow and suspended sediment to the tidal reach of Corte Madera Creek was measured at a USGS gaging station located above tidal influence at Ross, CA—Corte Madera Creek at Ross, CA (Site 11460000, http://waterdata.usgs.gov/nwis, Fig. 1). This gaging station is located 6.4 km upstream of the mouth of the creek and has a drainage area of 47 km^2. Available data at this site were daily mean discharge values of both flow and suspended-sediment for the period November 1, 2009–May 31, 2010.

3.4. Analysis

Variations in suspended-sediment dynamics on tidal and seasonal timescales were analyzed using techniques of tidal phase averaging, flux decomposition, and quadrant analysis.

3.4.1. Periods of analysis

For both wet and dry seasons, two periods (each denoted as "Period") of approximately two weeks duration having continuous data for discharge and concentration at the Mouth station were identified (Table 1). Two week periods were selected to capture tidal variations associated with the spring-neap cycle. The wet periods were selected to encompass multiple precipitation events. Gaps in data records less than 3 h were filled using linear interpolation.

3.4.2. Tidal phase averaging

For each Period, instantaneous values of both velocity and suspended-sediment concentration at the Mouth station were used to calculate mean values as a function of tidal phase. Tidal phase was determined using mean channel velocity (V_a). The time of measurement was converted from calendar day to tidal phase using the following equation:

$$\theta_i = \frac{t_i - t_{s1}}{t_{s2} - t_{s1}} \cdot 360, \quad (1)$$

where θ_i is the tidal phase in degrees at time t_i of tidal cycle i. For each tidal cycle, slack after flood (0°) and subsequent slack after flood (360°) are t_{S1} and t_{S2}, respectively. Ebb tides ($V_a > 0$) occur between approximately 0 and 180°; slack after ebb does not occur at exactly 180° due to variable tidal cycle durations. Data were linearly interpolated onto and averaged over phase bins of 0.05°. Velocity and SSC values within the same phase

Table 1
Periods from 2010 used in analysis.

Period	Dates	Season	Tidal cycles
W1	20 Feb–6 Mar	Wet	30
W2	3 Apr–17 Apr	Wet	27
D1	27 Jun–10 Jul	Dry	27
D2	1 Oct–17 Oct	Dry	29

bin were averaged together to determine mean V_a and C over the tidal cycle; comparisons were made between wet and dry seasons.

3.4.3. Flux decomposition

Suspended-sediment flux at the Mouth station was decomposed according to Dyer (1974), assuming lateral and vertical variations in SSC are captured by channel-average SSC (C):

$$[Q_s] = \underset{(1)}{[[V_a][A][C]]} + \underset{(2)}{[V'_a[A][C]]} + \underset{(3)}{[[V_a]A'[C]]} + \underset{(4)}{[V'_aA'[C]]} + \underset{(5)}{[[V_a][A]C']} + \underset{(6)}{[V'_a[A]C']} + \underset{(7)}{[[V_a]A'C']} + \underset{(8)}{[V'_aA'C']}, \quad (2)$$

where brackets indicate tidally averaged values and prime denotes deviations of instantaneous values from tidally averaged values (fluctuations), i.e., $C' = C - [C]$. Tidal averaging was performed using a low-pass Butterworth filter with a 30-hour stop period and a 40-hour pass period. This filtering process retains tidal variations with periods greater than 30 h, such as the spring-neap cycle.

In this analysis, we expect the most important contributors to total flux are the advective, dispersive, and Stokes drift terms (Eq. (2) right-hand side terms 1, 6, and 4, respectively), as shown by Ganju and Schoellhamer (2006). The advective flux term describes the contribution of tidally averaged values of discharge and concentration, assumed to be caused by discharge from Corte Madera Creek. The dispersive flux term describes the correlation of fluctuating values of velocity and concentration. Finally, the Stokes drift term describes the correlation of fluctuating values of velocity and area.

3.4.4. Quadrant analysis

Quadrant analysis was performed to summarize and compare seasonal differences in the dynamics contributing to suspended-sediment flux at the Mouth station. The magnitude and direction of suspended-sediment flux in a tidal creek are expected to vary seasonally. During rain events, runoff from the watershed will carry suspended sediment into the tidal reach; some fraction of this material will be transported to the estuary, depending on effects from tidal interactions. In between rain events, suspended-sediment flux is expected to be lower in magnitude, but the direction will depend on other processes such as flood-ebb asymmetry, spring-neap tidal cycle, and wind–wave resuspension. To discern seasonal variations in sediment transport at the Mouth station, a quadrant analysis was performed for wet and dry Periods. Consider the plane created by plotting mean channel velocity, V_a, against mean channel SSC fluctuation, C'. The classification of the quadrants of this plane is based on the signs of V_a and C' as follows (Fig. 2):

- Quadrant TE: turbid ebb, q_{TE} ($V_a > 0$, $C' > 0$);
- Quadrant TF: turbid flood, q_{TF} ($V_a < 0$, $C' > 0$);
- Quadrant CF: clear flood, q_{CF} ($V_a < 0$, $C' < 0$);
- Quadrant CE: clear ebb, q_{CE} ($V_a > 0$, $C' < 0$).

The sign on fluctuating concentration (C') represents the SSC of the water relative to subtidal conditions; positive C' indicates higher than average SSC (relatively turbid waters) while negative C' indicates lower than average SSC (relatively clear waters). An example of a C' time series is shown for Period W1 in Fig. 3. The mean suspended-sediment flux in each quadrant q for each Period is calculated as follows:

$$\overline{Q_{s,q}} = \frac{1}{n}\sum_0^n S_Q(t)V_a(t)C(t)A(t), \quad (3)$$

where the overbar indicates the mean over the duration of the Period comprising n values (Table 1) and $S_Q(t)$ is the averaging condition,

$$S_Q(t) = \begin{cases} 1, & \text{if } [V_a(t), C(t)] \text{ is in } q\text{th quadrant} \\ 0, & \text{otherwise} \end{cases} \quad (4)$$

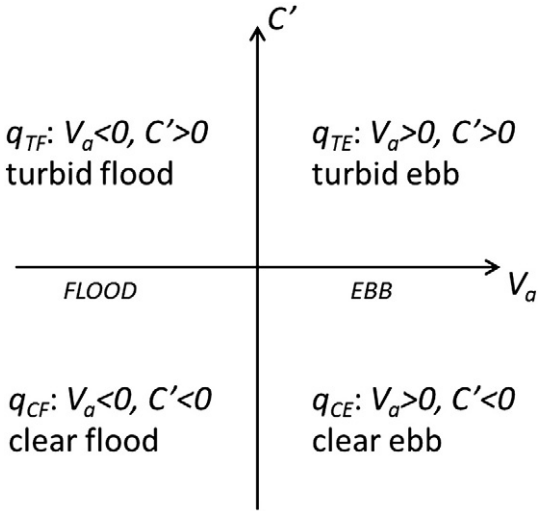

Fig. 2. Delineation of quadrants used to identify sediment transport events in quadrant analysis. Events are categorized by the direction of velocity V_a (flood vs. ebb) and the magnitude of concentration relative to tidally-averaged conditions, represented by the sign of fluctuating channel average suspended-sediment concentration C' (relatively turbid vs. relatively clear).

This analysis is based on turbulence studies (e.g., Lu and Willmarth, 1973) and provides both a tool for summarizing V_a and C time series and a quantitative measure of the relative importance of tidal phase and fluctuating SSC on the total suspended-sediment flux.

4. Results

4.1. Continuous record development

Measurements of instantaneous channel discharge ($n = 378$) were collected on both flood and ebb tides over a range of channel velocities. The stage–area relationship was calculated using bathymetry from the transect taken at the highest stage during hydroboard/kayak measurements; this stage was in the 95th percentile of observed stage measurements. The resulting relation between stage and cross-sectional area was:

$$A = 4.59(S)^2 + 49.2(S) + 64.6, \quad (5)$$

where A is the channel cross-sectional area (in m^2) and S is the stage recorded at the gaging station (in m). Similar relations were developed from four other transects: one other from the hydroboard-mounted ADCP and three from the boat-mounted ADCP. These relations were compared to determine variability in the stage–area fitting; a root-mean-square (RMS) error of 5.7 m^2 was observed; when expressed as mean percent deviation of measured values from predicted values, the error is 4%. The calibration curve for V_a as a function of V_i (Fig. 4) demonstrated a nearly 1:1 relation and had a RMS error of 0.043 m s^{-1} or 20% when expressed as mean percent deviation. The relation between turbidity and C (Fig. 5) showed increased scatter at higher values of turbidity and had a RMS error of 54 mg L^{-1} or 19% when expressed as mean percent deviation. Error in net flux measurement for all periods was calculated by summing in quadrature the mean percent deviations for the three calibration curves, yielding 28%.

To assess the presence of a velocity bias that could affect total flux calculations, we calculated the net water flux for an extended period with no rain (6/25/10–10/17/10, 113 days). Although discharge was not measured at Ross during this period, we assume negligible discharge enters the tidal reach from upstream; mean discharge at Ross for the months of July through October during 1951–1993 was 0.035 m^3 s^{-1} (USGS, 2011). For no net inflow into and no losses within the tidal reach, we expect the net water flux at the Mouth to

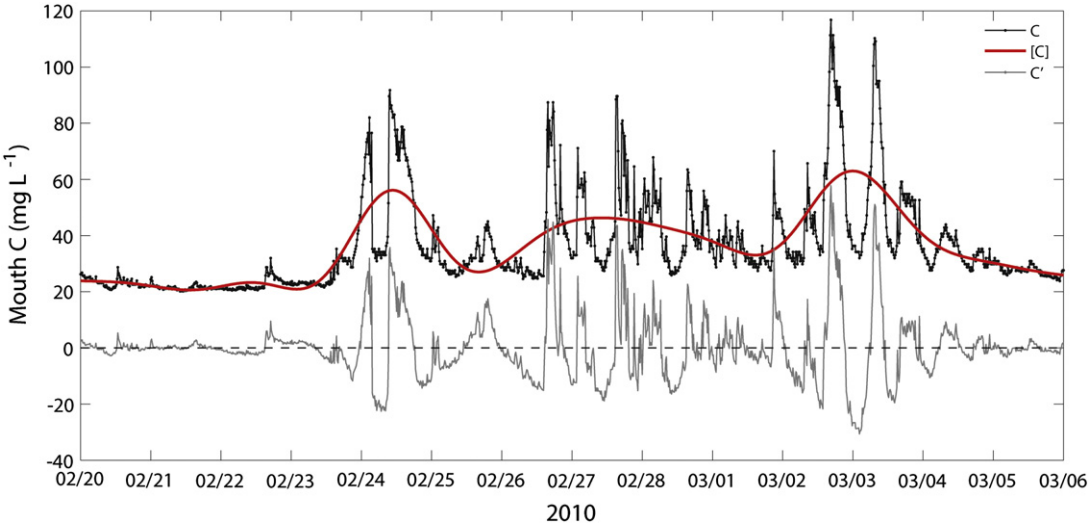

Fig. 3. Example time series of instantaneous (C), tidally averaged ([C]), and fluctuating (C') channel average SSC at the Mouth during Period W1 (wet season).

be zero. For this period, the net water flux was 4.5e6 m^3 (outflow), which implies a residual seaward discharge of 0.48 $m^3\ s^{-1}$. Assuming an average channel area of 140 m^2, this leads to a seaward velocity bias of 0.35 cm s^{-1}, which is within the accuracy of the ADVM (specified as 1% of measured velocity $\pm$0.5 cm s^{-1}).

4.2. Wet season time series

During both wet season Periods (W1 and W2), net suspended-sediment flux at the Mouth was seaward. Discharge of suspended-sediment from the watershed followed precipitation events, as observed at Ross during Period W1 (Fig. 6a). At the Mouth, a semidiurnal velocity pattern is evident with an ebb-dominant current asymmetry (Fig. 6b). Highest concentrations of suspended sediment at the Mouth were observed on ebb tides during and immediately following storms (Fig. 6c). Suspended-sediment flux at the Mouth (Q_s) was generally seaward and corresponded to Ross suspended-sediment discharge (Fig. 6a and d), indicating that watershed-sourced suspended sediment was discharged through the tidal reach.

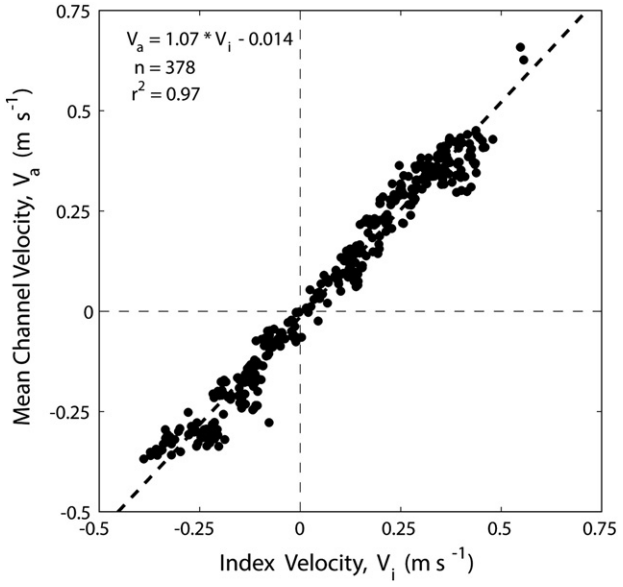

Fig. 4. Relation between index velocity (V_i) and mean channel velocity (V_a) at Mouth station. Positive values indicate seaward direction (ebb) and negative values indicate landward (flood) direction.

As observed at the Mouth, the conveyance of watershed-sourced sediment through the tidal reach was affected by tidal interactions (Fig. 6b–c). For example, the storm on 23 Feb 2010 caused suspended-sediment discharge from the upstream station, and part of this sediment pulse exited the tidal reach on the weak overnight ebb. On the subsequent flood tide (02:45–07:30 PST on 24 Feb 2010), transport of the sediment pulse through the tidal reach was halted and already-discharged sediment was not transported back into the tidal reach (observed as relatively low C during this flood tide). This suggests sediment discharged to the estuary does not return to the tidal reach on the subsequent floodtide. On the following ebb tide (07:30–16:30 PST on 24 Feb 2010), higher values of C indicate most of the watershed sediment pulse was discharged through the tidal reach during this strong ebb tide. It is expected that the flood tide during this storm reduced the amount of watershed sediment discharged to San Francisco Bay by reversing the direction of flow, thereby reducing channel velocity and allowing increased opportunity for settling within the tidal reach. This may account for the reduced magnitudes of suspended-sediment flux at the Mouth compared to the Ross station (Fig. 6a and d). Assuming this difference in flux between Mouth and Ross is due to settling within the tidal reach, we can estimate the net deposition during Period W1. Using an assumed bulk density of 1300 kg m^{-3} (Sternberg et al.,

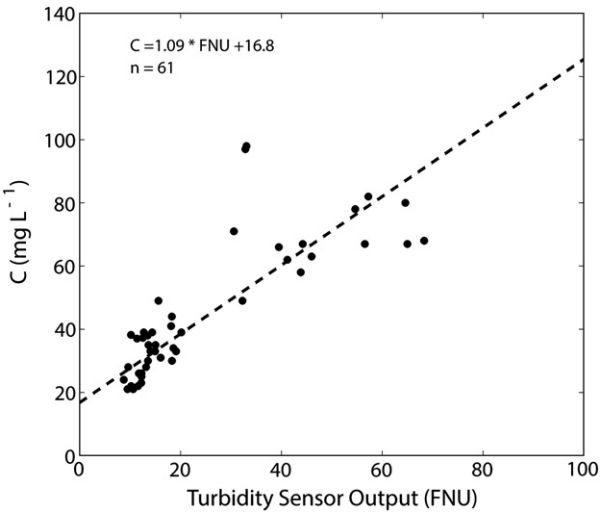

Fig. 5. Relation between turbidity sensor output and suspended-sediment concentration C at Mouth station.

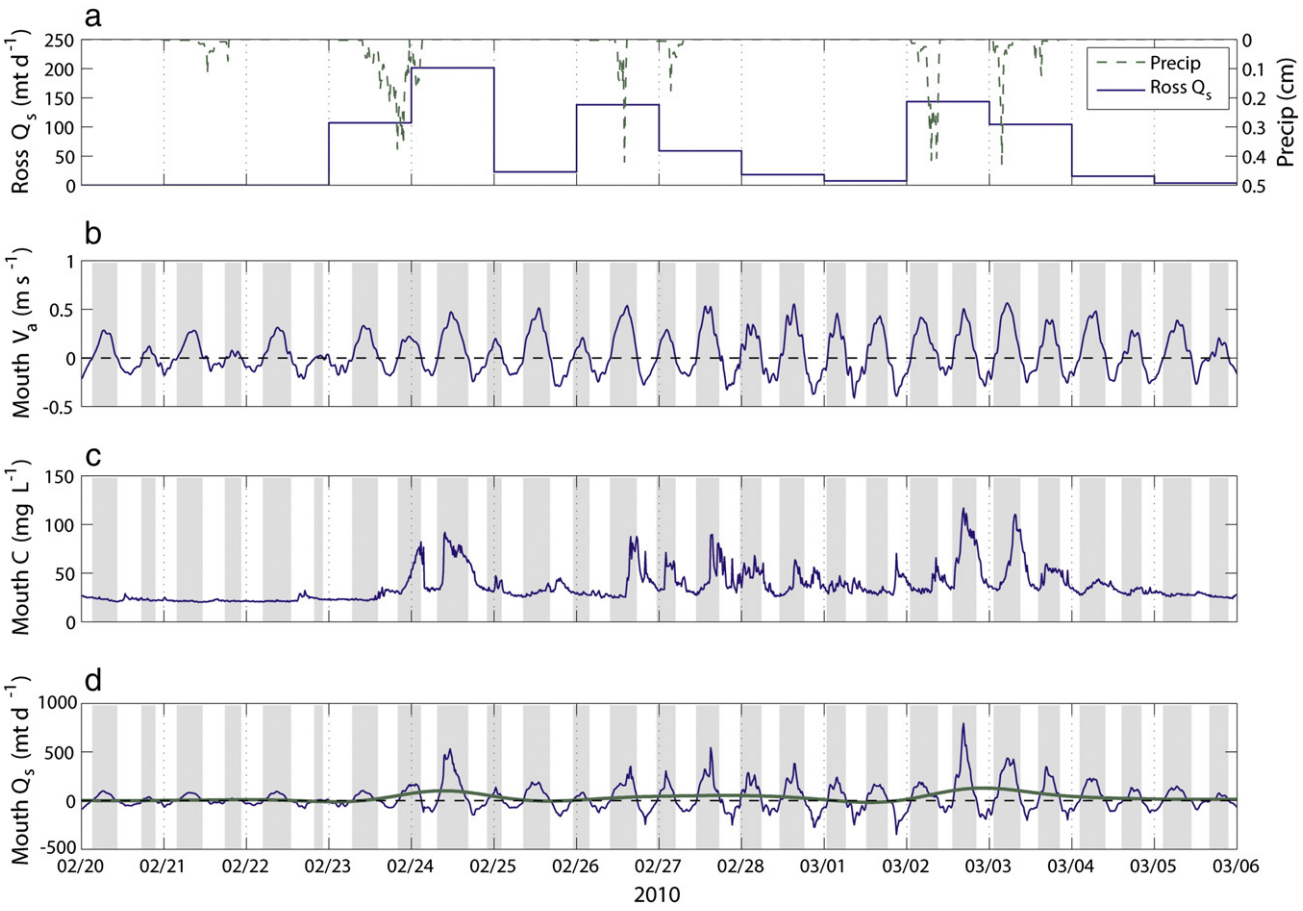

Fig. 6. Fourteen-day time series of period W1 during wet season. (a) Rain causes suspended-sediment discharge from the watershed (Ross Q_s), reported as daily mean values in metric tons. (b) Channel velocity at the Mouth station changes direction with the tides (positive values indicate ebb, denoted by shaded regions). (c) Channel suspended-sediment concentration at the Mouth increases on ebb tides following rainfall and watershed discharge. (d) Instantaneous suspended-sediment flux at the Mouth, Q_s, is generally seaward and is directly related to watershed inputs. Tidally averaged suspended-sediment flux, [Q_s], is shown by the thick solid line.

1986) and an area of the tidal reach of 4.1e5 m^2, the deposition is 0.06 cm during Period W1.

4.3. Dry season time series

During both dry season Periods (D1 and D2), net suspended-sediment flux at the Mouth station was landward, but with varying magnitude. In both Periods, a semidiurnal velocity pattern at the Mouth was evident with increasing magnitude during spring tides (Figs. 7a–b and 8a–b). In Period D1, highest magnitudes of suspended-sediment concentration at the Mouth were observed on nearly all afternoon flood tides (Fig. 7c). In contrast, for Period D2, highest magnitudes of both V_a and C at the Mouth were observed on spring flood tides (4 Oct 2010–10 Oct 2010, Fig. 8b–c). The maximum phase-averaged flood velocities observed were 0.16 m s^{-1} and 0.25 m s^{-1} for Periods D1 and D2, respectively (shown for D2 in Fig. 9b). On a tidal timescale, the timing of these C peaks coincided with peaks in flood velocity for both Periods (Figs. 7b c and 8b c); the shape of these Mouth C peaks was generally positively skewed with longer tails after the peak. The flood tide peaks in Mouth C were generally followed by smaller peaks on subsequent ebbs; ratios of flood peak C to subsequent ebb peak C ranged from 1.3 to 2.5. Assuming similar duration of floods and ebbs, this suggests net flux of sediment from the estuary into the tidal reach. This expectation is reflected in the generally landward direction of suspended-sediment flux (Qs) in both dry Periods (Figs. 7d and 8d); however, net tidally averaged suspended-sediment flux was nearly four times greater during Period D2 (190 ± 53 kg s^{-1} landward) than during Period D1 (49 ± 14 kg s^{-1} landward).

Different processes appear to have increased landward suspended-sediment flux during Periods D1 and D2. To identify the significant processes, peak suspended-sediment concentration (C) on each flood tide was compared with concurrent values of potential forcing factors. The factors we considered were wind–wave resuspension, inundation, local resuspension, and advection, estimated respectively as: wind speed at low slack tide (W_{lt}, taken as mean wind speed in the two-hour interval preceding slack tide at low water); stage at low slack tide (S_{lt}); maximum flood velocity (U_{max}); and tidal excursion from low slack tide to time of peak flood concentration (L, calculated as integral of velocity during time period from low slack tide to peak flood concentration). The relative importance of the forcing factors was not consistent between the two dry Periods (Table 2). During Period D1, the greatest correlation was between peak C and W_{lt} ($r = 0.47$, $p = 0.014$), indicating that increased winds near the end of ebb tides lead to higher peak C on subsequent flood tide. Mean wind speed during Period D1 (2.2 m s^{-1}) in June and July was higher than during Period D2 (1.4 m s^{-1}) in October, which is typical for San Francisco Bay (Conomos et al., 1985). Also significantly correlated with peak concentration during Period D1 was L ($r = 0.43$, $p = 0.025$), indicating that as tidal excursion increases, peak suspended-sediment concentration increases. The correlation between peak C and U_{max} ($r = 0.37$, $p = 0.056$) was nearly significant. These results suggest the importance of wind–wave resuspension in Corte Madera Bay and subsequent advection of higher-turbidity waters into the tidal reach of Corte Madera Creek. During Period D2, the greatest correlation was

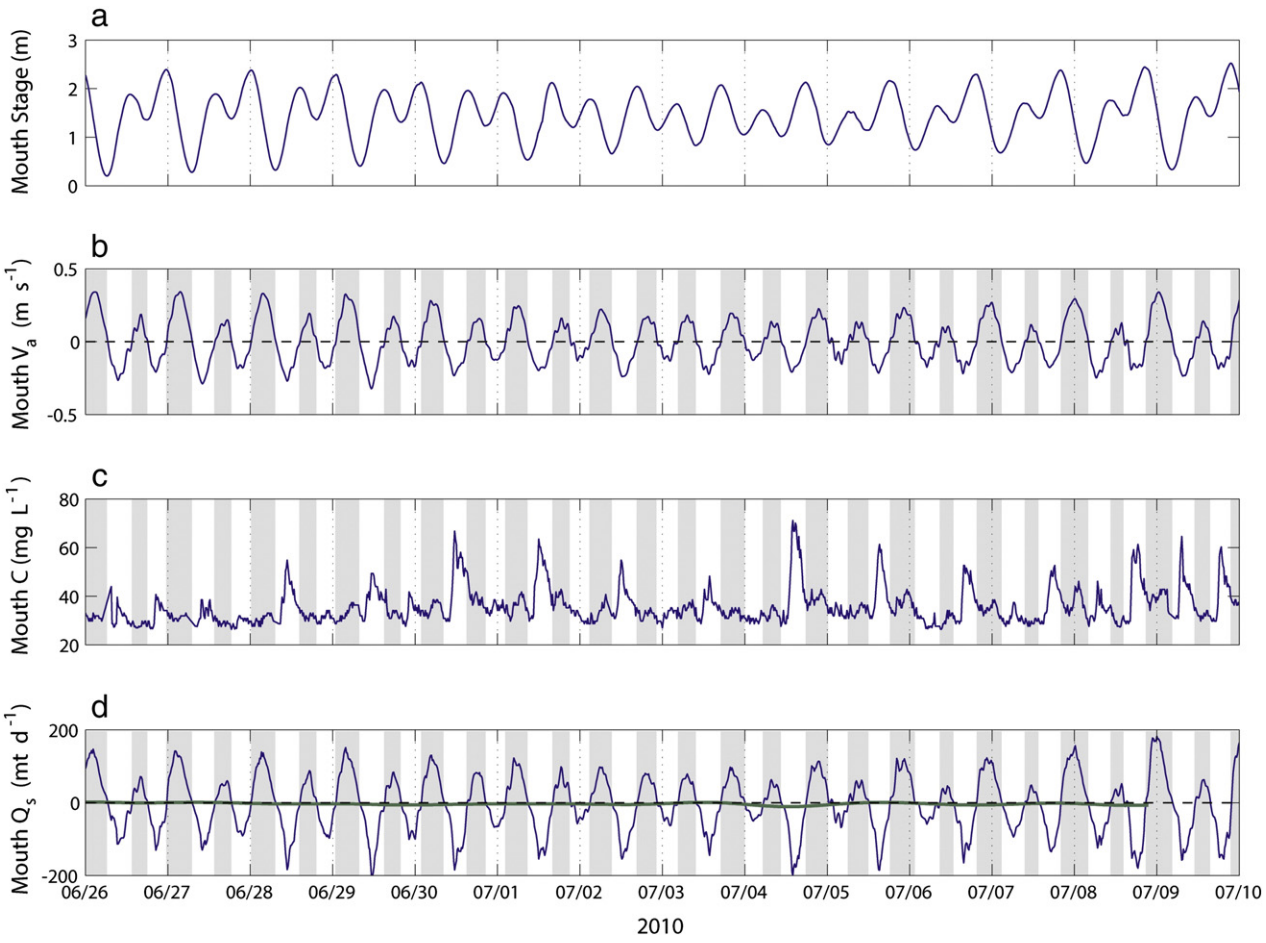

Fig. 7. Fourteen-day time series of Period D1 during dry season. (a) Stage at the Mouth varies with spring-neap cycle. (b) Channel velocity at the Mouth changes direction with the tides with a magnitude that also varies with spring-neap cycle. (c) Channel suspended-sediment concentration at the mouth increases on flood tides, with highest magnitudes during afternoon flood tides. (d) Instantaneous suspended-sediment flux at the Mouth, Q_s, reported in metric tons per day, is generally negative for this period, indicating landward transport of sediment. Tidally averaged suspended-sediment flux, $[Q_s]$, is shown by the thick solid line.

between peak C and U_{max} ($r = 0.57$, $p = 0.0013$). This result suggests that local resuspension is occurring during spring flood tides. Stage at low tide was not well correlated with peak flood concentration during these Periods, suggesting inundation alone is not a strong factor.

4.4. Tidal phase averaging

Suspended-sediment concentrations and channel velocities at the Mouth station varied both as a function of tidal phase and seasonally. During Period W1 (wet season), the highest and lowest tidal phase-averaged concentrations occurred near the end of ebb tides (43 ± 9 mg L^{-1}) and near the end of flood tides (29 ± 2 mg L^{-1}), respectively; tidal phase-averaged channel velocities were ebb-dominant with peak ebb magnitude of 0.3 m s^{-1} (Fig. 9a). In contrast, during Period D2 (dry season), the highest tidal phase-averaged concentrations (45 ± 10 mg L^{-1}) occurred near the time of maximum flood velocity, with a smaller, secondary peak (35 ± 3 mg L^{-1}) near the time of maximum ebb velocity; channel velocities were symmetric with peak magnitudes of 0.25 m s^{-1} (Fig. 9b). Results for Periods W2 and D1 were similar to W1 and D2, respectively, and are omitted here for brevity. Although the timing of the peak tidal phase-averaged concentration varied seasonally, the magnitude was similar between wet and dry seasons (43 and 45 mg L^{-1}, respectively). Greater variability in tidal phase-averaged concentration was observed for the wet season. This is expected to be caused by the variable timing of precipitation relative to the tidal cycle.

4.5. Discharge and flux decomposition

Tidally averaged channel discharge and the relative importance of suspended-sediment flux components varied seasonally. During wet Periods, instantaneous discharge varied tidally and in response to watershed discharge; tidally averaged channel discharge was seaward (Fig. 10a). The largest component of the tidally averaged flux was the advective flux during both wet Periods, followed closely by the dispersive flux (shown for Period W1 in Fig. 10b; results were similar for W2). The direction of dispersive flux was generally seaward for both Periods (shown for W1 in Fig. 10b; results were similar for W2); this is attributed to the increased correlation of positive values of both fluctuating velocity and fluctuating concentration.

During dry Periods, instantaneous discharge varied tidally and in response to spring-neap variations; tidally averaged channel discharge was negligible (shown for Period D2 in Fig. 11a; results were similar for D1). Tidally averaged flux was landward; the largest component was the dispersive flux (shown for D2 in Fig. 11b; results were similar for D1). During Period D2, landward flux increased during spring tides. The landward direction of dispersive flux during these Periods is attributed to the increased correlation of negative values of fluctuating velocity with positive values of fluctuating concentration.

For all Periods, advective flux, dispersive flux, and Stokes drift flux accounted for more than 97% of the tidally averaged suspended-sediment flux (Figs. 10b and 11b). Stokes drift flux was landward during all Periods and constituted the following percentages of tidally

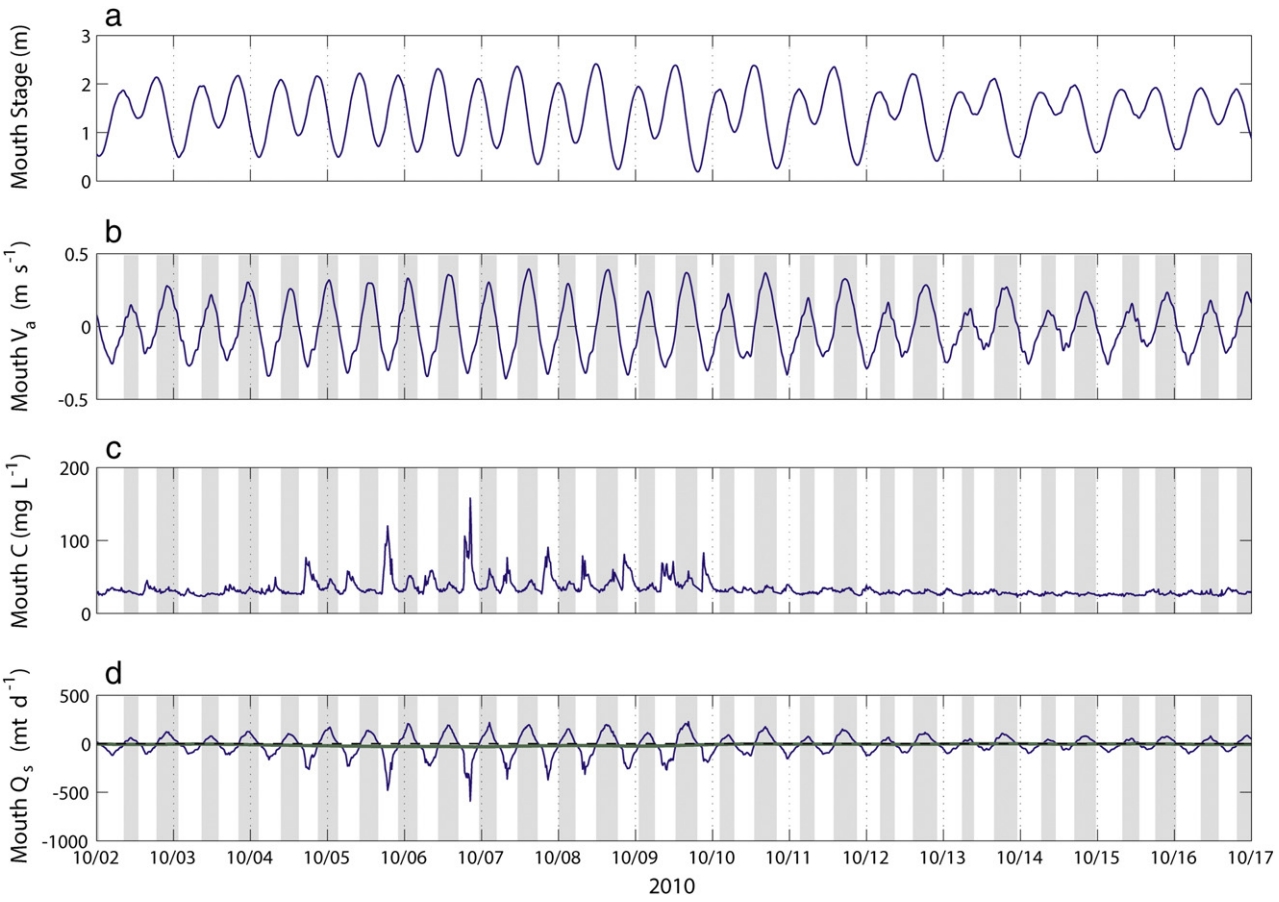

Fig. 8. Fifteen-day time series of Period D2 during dry season. (a) Stage at the Mouth varies with spring-neap cycle. (b) Channel velocity at the Mouth changes direction with the tides with a magnitude that also varies with spring-neap cycle. (c) Channel suspended-sediment concentration at the Mouth increases on flood tides, with highest magnitudes during periods of greatest flood velocity. (d) Instantaneous suspended-sediment flux at the Mouth, Q_s, reported in metric tons per day, is negative for this period, indicating landward transport of sediment. Tidally averaged suspended-sediment flux, $[Q_s]$, is shown by the thick solid line.

averaged flux for Periods W1, W2, D1, and D2, respectively: 12%; 11%; 10%; and 20%.

4.6. Quadrant analysis

Results of the quadrant analysis further highlight the seasonal variations in sediment transport and provide a method for summarizing suspended-sediment flux time series. As seen in Table 3, suspended-sediment flux occurs in all quadrants with varying magnitudes, demonstrating that sediment is transported into and out of the tidal reach with the tides. By comparing the relative magnitudes of mean suspended-sediment flux in each quadrant, the sediment transport processes that control suspended-sediment flux were identified for each Period. During wet Periods, mean suspended-sediment flux was greatest during turbid ebb tides (q_{TE}; 2.33 and 2.12 kg s^{-1} for Periods W1 and W2, respectively, Table 3). This implies most sediment was transported on ebb tides having higher than average suspended-sediment concentrations. In contrast, during dry Periods, mean suspended-sediment flux was greatest during turbid flood tides (q_{TF}; −1.29 and −1.67 kg s^{-1} for Periods D1 and D2, respectively, Table 3). This implies most sediment was transported on flood tides having higher than average SSC and suggests net import of sediment into the tidal reach.

5. Discussion

Our results indicate that the tidal reach of Corte Madera Creek is annually a net source of suspended sediment to San Francisco Bay but becomes a sediment sink in the dry season. The direction of tidally averaged suspended-sediment flux was seaward during wet periods and landward during dry periods (Figs. 6d, 7d, and 8d). Net tidally averaged suspended-sediment flux was greater in magnitude during wet periods (480 ± 130 and 370 ± 100 kg s^{-1} seaward for Periods W1 and W2, respectively). During dry periods, net tidally-averaged suspended-sediment flux during Period D1 (49 ± 14 kg s^{-1} landward) was 10% and 13% of that observed during Periods W1 and W2, respectively. During Period D2 (190 ± 53 kg s^{-1} landward), net flux was 40% and 51% of that observed during Periods W1 and W2, respectively. The fate of sediment transported into the tidal reach in dry periods is unknown; it may be a seasonal deposit that is remobilized and exported during subsequent wet periods, which would not affect net sediment supply on an annual timescale. However, this landward-transported sediment may also become a permanent deposit, which would reduce conveyance of watershed discharge by elevating the streambed, leading to increased risk of flooding. Regardless of its fate, this landward sediment flux affects the temporal availability of suspended sediment in the estuary on a seasonal timescale, which is relevant to management issues such as tidal wetland restoration, navigation, and shoreline protection.

Similar seasonal variations in suspended-sediment transport have been observed in other estuarine tributaries. In the Tavy sub-estuary of Tamar Estuary, Uncles and Stephens (2010) observed landward flux of suspended-sediment from early spring to late autumn and seaward flux during winter months, based on measurements of both suspended-sediment flux and bed elevation. In the Tavy, the landward flux was attributed to both reduced watershed discharge and increased wind–wave resuspension. Geyer et al. (2001) observed landward sediment flux at the mouth of the Hudson River estuary

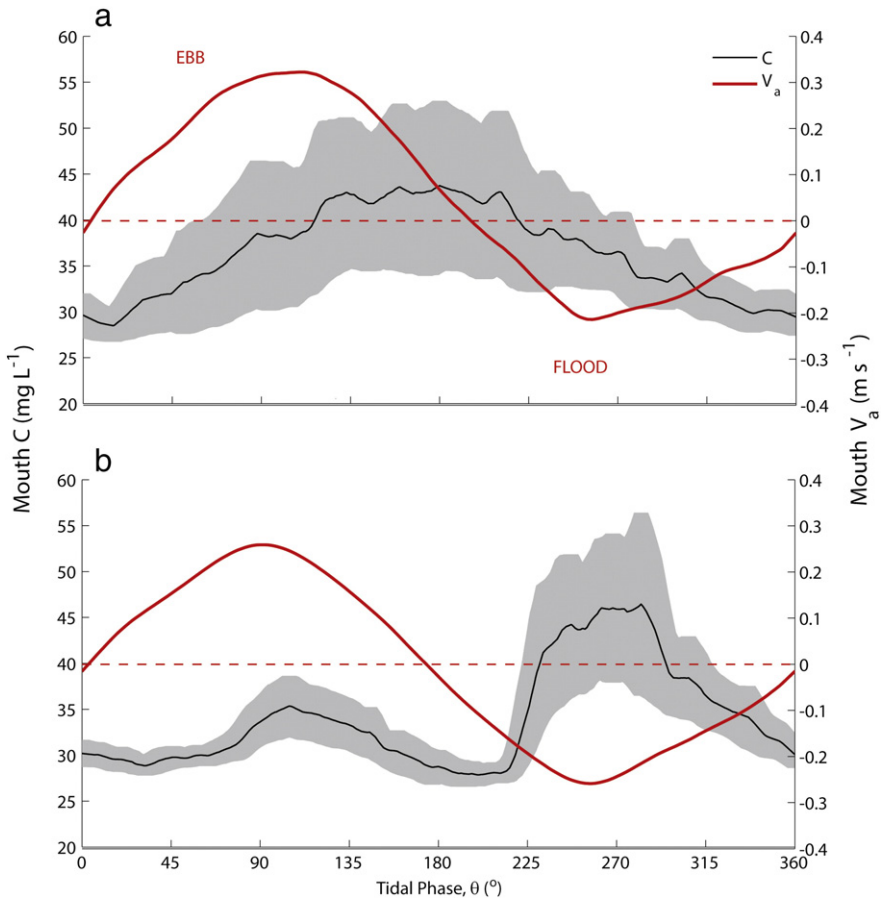

Fig. 9. Example of variation of average channel suspended-sediment concentrations at the Mouth as function of tidal phase (θ). (a) During wet season (Period W1 shown), highest concentrations are observed during later phase of ebb tides ($V_a > 0$ & $0 < \theta \leq 180$). (b) During dry season (Period D2 shown), highest concentrations are observed during flood tides ($V_a < 0$ & $180 < \theta \leq 360$). Shading denotes 95% confidence interval on the mean.

during late spring to mid-summer. They attributed the flux direction to watershed discharge and the flux magnitude to tidal amplitude, with increased landward transport occurring during periods of low watershed discharge coinciding with spring tide. In the Minas Basin, a subembayment of the Bay of Fundy, Greenberg and Amos (1983) observed accumulation of bottom sediments in the summer and subsequent erosion in the winter.

In other studies of river/estuary transitions, tidally oscillating sediment masses (discrete sediment masses that are resuspended and deposited each tidal cycle and transported upstream on floods and downstream on ebbs) were observed, creating turbidity zones (e.g., Uncles and Stephens, 1993; Grabemann and Krause, 1994; and Ganju et al., 2004). At Corte Madera Creek, only a fraction of the sediment mass exported from the watershed is observed to oscillate past the Mouth station during wet periods (Fig. 6); we expect this is because the mean tidal excursion on ebbs (3.6 km) is greater than the distance to the open waters of Corte Madera Bay (2 km), suggesting that sediments are transported to this sink during most tides. Visual observations confirm that watershed sediment plumes following storms are directed along the dredged navigation channel to these open waters. Subsequent flood tides are likely diluted by clearer Bay waters sourced from south of the navigation channel (Fig. 1), promoting sediment export to the estuary during the wet season.

The changing forcing factors for landward flux between dry Periods (Table 2) are attributed to changing wind conditions and velocity magnitudes. During the summer, when winds were higher, peak flood concentration was best correlated with both wind speed at low tide and tidal excursion (Period D1, Table 2). This suggests wind–wave resuspension in the estuary and subsequent advective transport during flood tides. Previous studies summarized by Schoellhamer et al. (2007) have found that wind–wave resuspension in shallow subembayments of San Francisco Bay is greatest in spring and summer and least in autumn due to seasonally varying winds and bed erodibility. Corte Madera Bay, the shallow subembayment seaward of the tributary under study, has been shown to have potential for wind–wave resuspension (Lacy and Hoover, 2011). In contrast, during autumn, peak flood velocity was the dominant factor in peak flood concentration (Period D2, Table 2), suggesting local resuspension during spring flood tides. We hypothesize that the C peaks are smaller on ebb than flood tides because of longitudinal bathymetric asymmetry. The dredged navigation

Table 2
Correlation coefficients (r) of forcing factors and peak flood concentrations for periods D1 and D2 (dry season). Wind speed was averaged over the 2 h preceding each slack tide at low water. Tidal excursion was calculated as the integral of velocity from low slack tide to the time of peak suspended-sediment concentration (C) observed.

Forcing factor	Definition	r_{D1}	r_{D2}
W_{lt}	Wind speed at low tide	0.47*	0.29
		$p = 0.014$	$p = 0.13$
S_{lt}	Stage at low tide	−0.18	−0.33
		$p = 0.37$	$p = 0.086$
U_{max}	Max flood velocity	0.37	0.57**
		$p = 0.056$	$p = 0.0013$
L	Tidal excursion from slack tide to peak C	0.43*	0.21
		$p = 0.025$	$p = 0.28$

*Statistically significant correlation at the 0.05 level; ** statistically significant correlation at the 0.01 level.

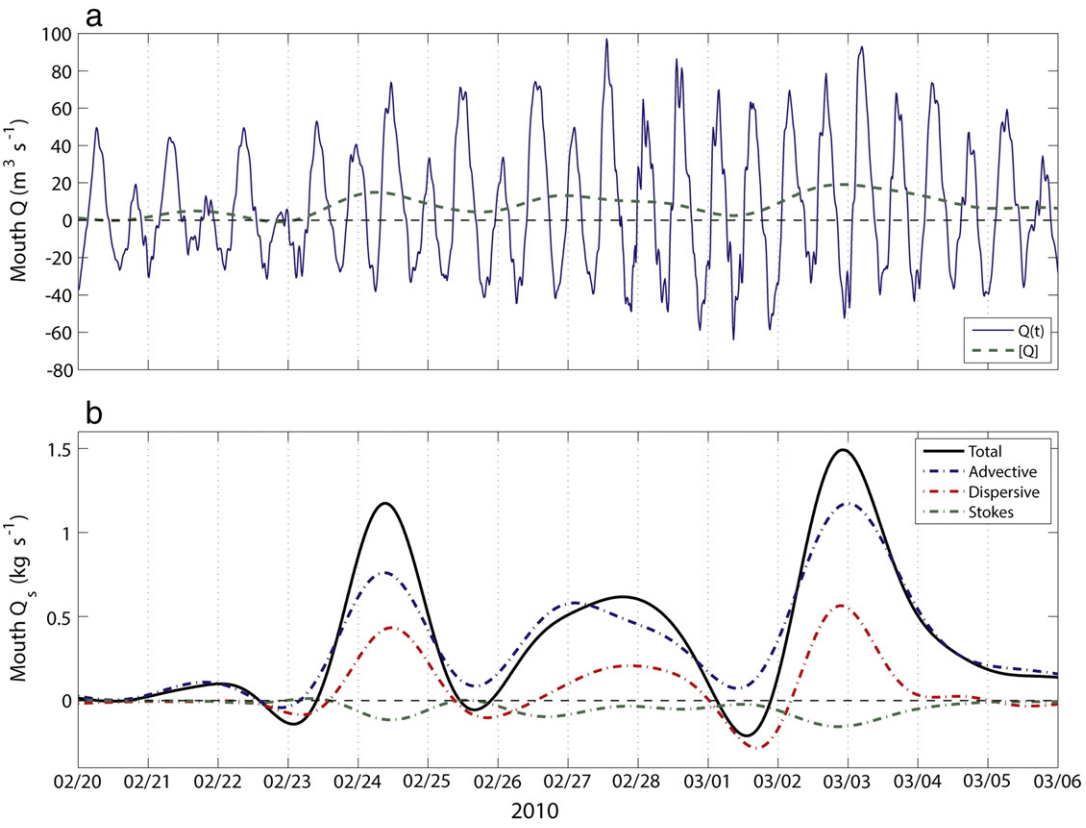

Fig. 10. Comparison of discharge (Q) and suspended-sediment flux (Q_s) at the Mouth during Period W1 (wet season). (a) Instantaneous and tidally averaged channel discharge; tidally averaged discharge is seaward, as expected given wet conditions with watershed discharge. (b) Tidally averaged suspended-sediment flux and components; advective flux dominates total flux during periods of watershed discharge. Dispersive flux is positive due to ebb-dominant tidal currents carrying higher SSC.

channel seaward of Mouth may provide a narrow and deep sediment sink at slack tide that is a concentrated source for resuspension on flood tide. The channel is wider and shallower landward of Mouth so deposition and subsequent resuspension may be more diffuse. We note that C is small when the diurnal inequality is relatively large, i.e., during neap tide (Fig. 8). A possible explanation is that the approximately 12 h of weak tides created by the diurnal inequality is sufficient time for consolidation to occur and reduce the supply of erodible sediment. The lower net suspended-sediment flux during Period D1 compared to D2 may be attributed to lower peak flood velocity, likely caused by weaker flood tide velocities during the summer compared to that during the autumn. Reduced tidal velocity is expected to cause decreases in both local resuspension and advective transport (by reducing tidal excursion). Thus we expect landward flux during dry periods is caused by a combination of advective transport of sediment resuspended by wind waves and local resuspension by increased flow velocities and bathymetric asymmetries.

During dry Periods, the dispersive flux was the largest component (shown for Period D2 in Fig. 11b); we expect the landward direction on dispersive flux during dry periods was caused by a longitudinal concentration gradient (dC/dx) with increasing SSC toward the estuary. We did not observe tidal velocity asymmetries (e.g., flood-dominant tidal currents; Figs. 7b and 8b), which have been shown elsewhere to cause landward flux (e.g., Friedrichs and Aubrey, 1988). We have not assessed vertical variations in suspended-sediment concentration or velocity, the presence of which would determine whether baroclinic estuarine circulation is a factor in the landward sediment flux (Schubel, 1968). However, given the negligible watershed discharge during the dry season (discussed in Section 4.1), we expect this process was not a factor in the observed landward flux. Despite the small bias in the index velocity relationship (described in Section 4.1), the dispersive flux dominates during dry season (Fig. 11b) and does not affect the interpretation of these results.

5.1. Quadrant analysis

The quadrant analysis presented here provides a method for summarizing time series of suspended-sediment flux by quantifying the relative importance of different sediment transport events. Sediment transport events are categorized by two factors: whether "the tide is ebb or flood" and whether the concentration is relatively turbid ($C' > 0$) or relatively clear ($C' < 0$) (Fig. 2). We found that during wet periods, suspended-sediment flux was greatest in magnitude during relatively turbid ebb tides (q_{TE}, Table 3), while during dry periods it was greatest in magnitude during relatively turbid flood tides (q_{TF}, Table 3). In addition, the relative importance of sediment transport events within each Period was consistent for each season, based on the equivalent rankings of the four quadrants for W1–W2 and D1–D2.

The similarities between the wet and dry Periods suggest that a conceptual model can characterize the quadrant analysis results seasonally. For the base case, where suspended-sediment transport is independent of the tidal velocity, we would expect the data to fall symmetrically along the $C' = 0$ line, as illustrated in case 1 of Fig. 12. For this case, the dispersive component of suspended-sediment flux would be zero. On a seasonal timescale, we observed differences in the direction of net suspended-sediment flux between wet season and dry seasons, which were seaward and landward, respectively. Conceptually, net seaward flux can be accomplished by the predominance of relatively turbid ebbs (q_{TE}) and/or relatively clear floods (q_{CF}). Similarly, net landward flux can be accomplished by the predominance of relatively turbid floods (q_{TF}) and/or relatively clear ebbs (q_{CE}). These are illustrated in cases 2 and 3 of Fig. 12, respectively.

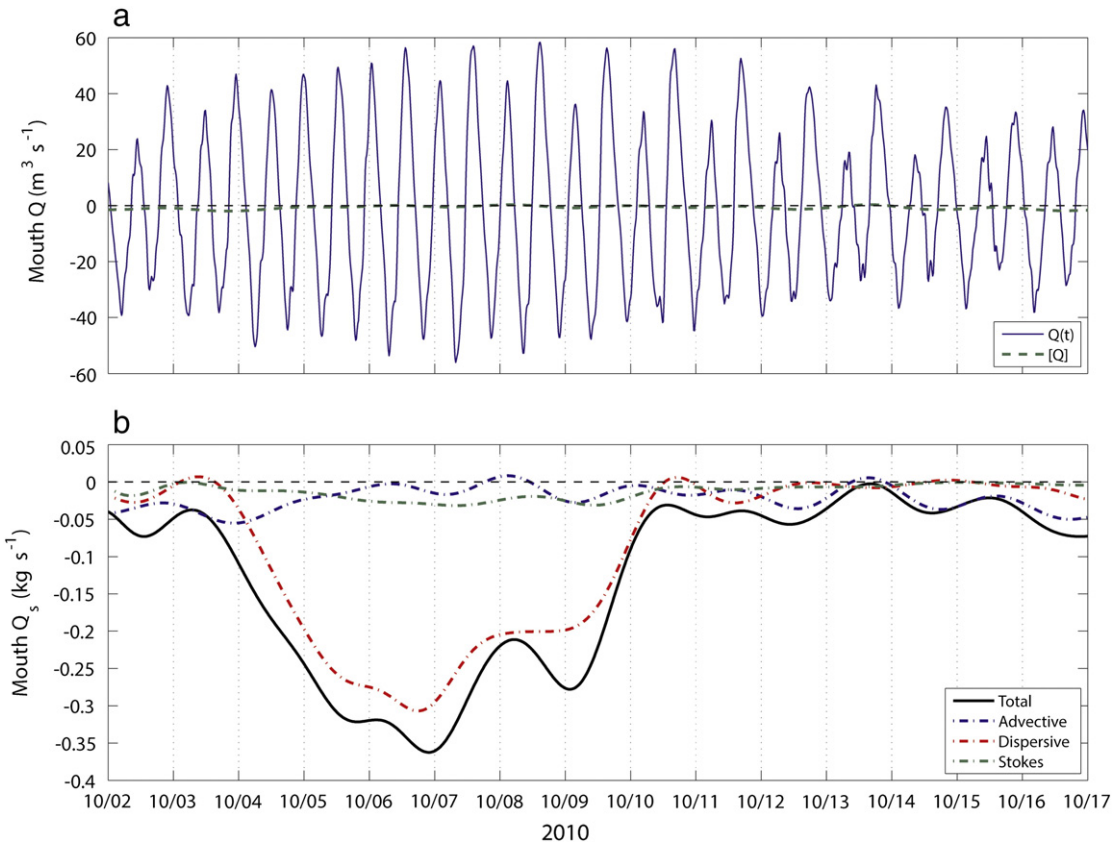

Fig. 11. Comparison of discharge (Q) and suspended-sediment flux (Q_s) at the Mouth during Period D2 (dry season). (a) Instantaneous and tidally averaged channel discharge; tidally averaged discharge is negligible, as expected given dry conditions with no watershed discharge. (b) Tidally averaged suspended-sediment flux and components; increased landward flux is observed during spring tide. Dispersive flux dominates total flux during dry season due to increased SSC on flood tides.

This conceptual model was applied to Periods W1 and D2 for illustration purposes. The centroid of each quadrant was computed as the mean values in each quadrant, i.e., $\left(\overline{U}, \overline{C}'\right)$. During Period W1, the greatest values of $|\overline{U}|$ and $|\overline{C}'|$ are found in q_{TE} (Fig. 13a), indicating that turbid ebb tides predominate and sediment flux is seaward. During Period D2, the greatest values of $|\overline{U}|$ and $|\overline{C}'|$ were found in q_{TF} (Fig. 13b), indicating that turbid flood tides predominate and sediment flux is landward.

For both wet and dry Periods, the majority of the data fall along $C' = 0$ (i.e., $|\overline{C}'|$ is small), suggesting that suspended-sediment flux is dominated by relatively few, large events. During the wet season, these events are storms that cause increased suspended-sediment discharge from the watershed, which exits the tidal reach on turbid ebbs. During the dry season, these events are turbid floods, caused by processes such as spring tides that cause local resuspension (as for Period D2, Fig. 8) or wind–wave resuspension of sediment in the estuary and subsequent flood tide advection into the tidal reach. These findings are corroborated by the time series analysis and the tidal phase averaging; thus this technique provides a convenient method for summarizing suspended-sediment flux time series.

Table 3
Quadrant analysis results for the Mouth station, depicting mean of instantaneous suspended-sediment flux $\left(\overline{Q_{s,q}}\right)$ in each quadrant; positive values indicate seaward transport. During wet periods, turbid ebbs (q_{TE}) dominate sediment transport, indicating seaward sediment transport out of the tidal reach. In contrast, during dry periods, turbid floods (q_{TF}) dominate, indicating landward sediment transport into the tidal reach from the estuary.

		$\left(\overline{Q_{s,q}}\right)$ (kg s^{-1})			
Period	Season	q_{TE}	q_{TF}	q_{CF}	q_{CE}
W1	Wet	2.33	−0.90	−0.70	0.92
W2	Wet	2.12	−0.97	−0.53	0.78
D1	Dry	0.89	−1.29	−0.43	0.61
D2	Dry	1.01	−1.67	−0.44	0.66

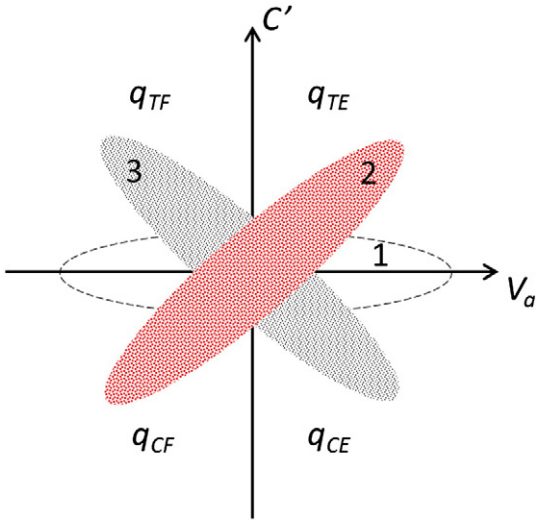

Fig. 12. Schematic of expected quadrant analysis results for the cases where (1) sediment transport is independent of tidal velocity (dashed ellipse); (2) net seaward sediment transport (red-dotted ellipse); and (3) net landward sediment transport (black-dotted ellipse). For net seaward transport, both turbid ebbs and clear floods are expected to dominate sediment flux, whereas, for net landward transport, both turbid floods and clear ebbs are expected to dominate. Ellipses represent an idealized representation of the distribution of data points. Quadrants are defined in Fig. 2.

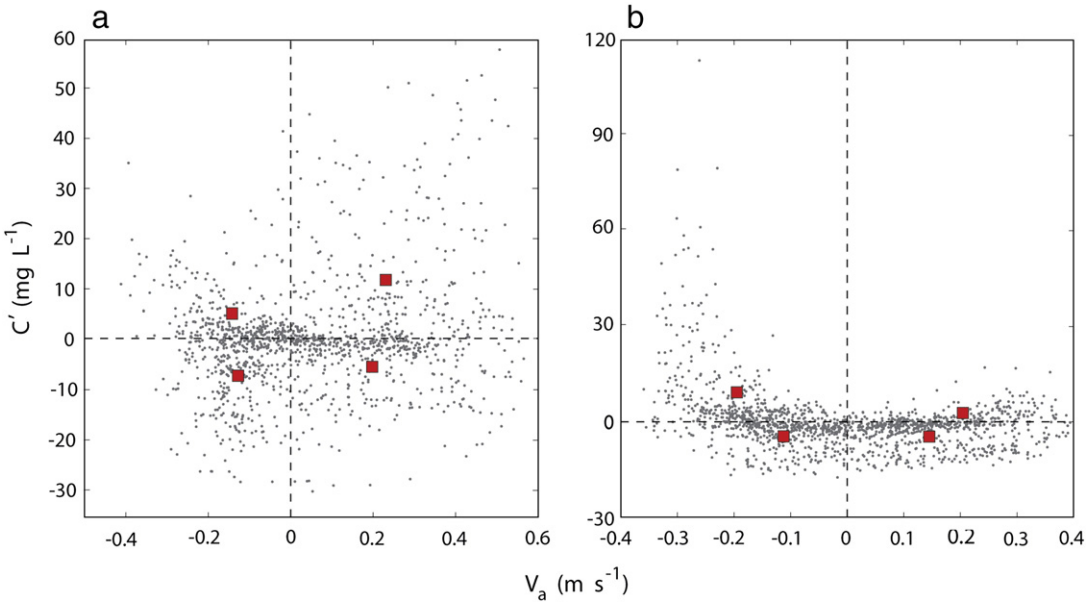

Fig. 13. Quadrant analysis results for (a) Period W1 (wet season) and (b) Period D2 (dry season). Filled squares denote centroid $\left(\overline{V}_a, \overline{C}'\right)$ of each quadrant. The largest values of $|\overline{V}_a|$ and $\left|\overline{C}'\right|$ are found in q_{TE} during the wet season and in q_{TF} during the dry season. Quadrants are defined in Fig. 2.

5.2. Implications

This study demonstrates seasonal variations in suspended-sediment dynamics in the tidal reach of an estuarine tributary in San Francisco Bay. We have observed important processes that trap suspended sediments in this tidal reach, including attenuation of suspended-sediment flux from the watershed during the wet season (Fig. 6) and landward transport of suspended-sediment during the dry season (Figs. 7 and 8). Existing studies of sediment supply to the open waters of San Francisco Bay from local tributaries are based on measurements made above tidal influence and thus have not accounted for effects of tidal reaches (e.g., Porterfield, 1980; Lewicki and McKee, 2009). Given the similar hydrologic setting of other local tributaries to that of the present study, we expect them to have similar sediment transport characteristics. Thus, existing calculations of estuary sediment supply from local tributaries may be overestimates because they do not account for potential trapping processes in the tidal reach. Local bathymetry, however, is an important factor for determining sediment transport characteristics. For example, proximity to shallow water subembayments of the estuary is expected to be an important factor in whether the tidal reach will become a sediment sink. Increased wind–wave resuspension in shallow subembayments is expected to increase the longitudinal concentration gradient, leading to increased landward flux into the tidal reach by dispersive processes. Additionally, proximity to permanent sediment sinks is expected to control the development of oscillating sediment masses. Restoration projects that rely on availability of suspended sediment (e.g., tidal wetlands) located along or near tidal reaches of estuarine tributaries should consider seasonal variations in sediment dynamics. These results highlight the importance of defining estuary boundaries in sediment budget calculations and the need for consistent definitions of these boundaries across studies. Further understanding of the sediment budget within tidal reaches of estuarine tributaries at annual timescales is needed. The processes observed in this study give cause for reexamining existing sediment budgets for this and similar estuaries.

6. Conclusions

Seasonal variations in suspended-sediment flux have been observed in the tidal reach of an estuarine tributary. Seaward suspended-sediment flux occurs during the wet season and is dominated by advective processes. In contrast, landward suspended-sediment flux occurs during the dry season and is dominated by dispersive processes. Landward flux appears to be caused by both increased flow velocities during spring tides and wind–wave resuspension in the estuary. Thus, during the dry season, local tributaries likely are sediment sinks, thereby reducing the availability of suspended sediment in the estuary. A quadrant analysis is proposed to summarize and compare seasonal differences in suspended-sediment dynamics. This analysis demonstrates the importance of few, relatively large events on net suspended-sediment flux, and provides a tool for summarizing flux time series. These results suggest that existing estimates of sediment supply to San Francisco Bay from local tributaries may be biased by not accounting for the tidal reach, which acts to both attenuate sediment pulses from the watershed and capture suspended sediment from San Francisco Bay during the dry season.

Acknowledgments

This study was supported by the U.S. Army Corps of Engineers, San Francisco District, as part of a Regional Sediment Management Program for San Francisco Bay. We also thank the San Francisco Bay Conservation and Development Commission for their assistance. We thank Paul Buchanan, Amber Forest, Lissa MacVean, Tara Morgan, Greg Shellenbarger, Kurt Weidich, Brooks Weisser, Dan Whealdon-Haught, Wayne Wagner, Rob Wilson, and Scott Wright for their assistance with data collection and analysis. We thank Greg Shellenbarger, John Warner, and two anonymous reviewers for reviewing this manuscript.

References

Conomos, T.J., Smith, R.E., Gartner, J.W., 1985. Environmental setting of San Francisco Bay. Hydrobiologia 129, 1–12.
Dyer, K.R., 1974. The salt balance in stratified estuaries. Estuarine and Coastal Marine Science 2, 273–281.
Edwards, T.K., Glysson, G.D., 1999. Field methods for measurement of fluvial sediment. U.S Geological Survey Techniques of Water-Resource Investigations, book 3, Applications of Hydraulics, chap. C2 (rev.) (89 pp. Available at http://pubs.usgs.gov/twri/twri3-c2/).
Friedrichs, C.T., Aubrey, D.G., 1988. Non-linear tidal distortion in shallow well-mixed estuaries: a synthesis. Estuarine, Coastal and Shelf Science 27, 521–545.
Ganju, N.K., Schoellhamer, D.H., 2006. Annual sediment flux estimates in a tidal strait using surrogate measurements. Estuarine, Coastal and Shelf Science 69, 165–178.

Ganju, N.K., Schoellhamer, D.H., Warner, J.C., Barad, M.F., Schladow, S.G., 2004. Tidal oscillation of sediment between a river and a bay: a conceptual model. Estuarine, Coastal and Shelf Science 60, 81–90.

Geyer, W.R., Woodruff, J.D., Traykovski, P., 2001. Sediment transport and trapping in the Hudson River Estuary. Estuaries 24, 670–679.

Grabemann, I., Krause, G., 1994. Suspended matter fluxes in the turbidity maximum of the Weser Estuary. In: Dyer, K.R., Orth, R.J. (Eds.), Changes in Fluxes in Estuaries. Olsen & Olsen, Denmark, pp. 23–28.

Greenberg, D.A., Amos, C.L., 1983. Suspended sediment transport and deposition modeling in the Bay of Fundy, Nova Scotia: a region of potential tidal power development. Canadian Journal of Fisheries and Aquatic Sciences 40 (Suppl. 1), 20–34.

Kroll, C.G., 1975. Estimate of sediment discharges, Santa Ana River at Santa Ana and Santa Maria River at Guadalupe California. U.S. Geological Survey Water-Resources Investigations, 40–74 (18 pp.).

Lacy, J.R., Hoover, D.J., 2011. Wave exposure of Corte Madera Marsh, Marin County, California — a field investigation. U.S. Geological Survey Open-File Report, 2011–1183 (28 pp. Available at http://pubs.usgs.gov/of/2011/1183/).

Lewicki, M., McKee, L., 2009. Watershed specific and regional scale suspended sediment loads for Bay Area small tributaries. A technical report for the Sources Pathways and Loading Workgroup of the Regional Monitoring Program for Water Quality: SFEI Contribution, 566. San Francisco Estuary Institute, Oakland, CA (56 pp.).

Lu, S.S., Willmarth, W.W., 1973. Measurements of the structure of the Reynolds stress in a turbulent boundary layer. Journal of Fluid Mechanics 60, 481–511.

McKee, L., Leatherbarrow, J., Pearce, S., Davis, J., 2003. A review of urban runoff processes in the Bay Area: existing knowledge, conceptual models, and monitoring recommendations. A report prepared for the Sources. Pathways and Loading Workgroup of the Regional Monitoring Program for Trace Substances. : SFEI Contribution, 66. San Francisco Estuary Institute, Oakland, CA.

McKee, L.J., Lewicki, M., Schoellhamer, D.H., Ganju, N.K., 2013. Comparison of sediment supply to San Francisco Bay from Coastal and Sierra Nevada watersheds. Marine Geology, Special Issue on San Francisco Bay 345, 47–62 (this issue).

Porterfield, G., 1980. Sediment transport of streams tributary to San Francisco, San Pablo, and Suisun Bays, California, 1909–1966. U.S. Geological Survey Water-Resources Investigations 80–64, 91pp.

Ruhl, C.A., Simpson, M.R., 2005. Computation of discharge using the index-velocity method in tidally affected areas. U.S. Geological Survey Scientific Investigations Report, 2005–5004 (31 pp.).

Schoellhamer, D.H., Mumley, T.E., Leatherbarrow, J.E., 2007. Suspended sediment and sediment-associated contaminants in San Francisco Bay. Environmental Research 105, 119–131.

Schubel, J.R., 1968. Turbidity maximum of the northern Chesapeake Bay. Science 6, 1012–1015.

Schubel, J.R., Carter, H.H., 1976. Suspended sediment budget for Chesapeake Bay. In: Wiley, M. (Ed.), Estuarine Processes, Vol. 2. Academic Press, New York, pp. 48–62.

Siegel, A.R., 1982. Robust regression using repeated medians. Biometrika 69, 242–244.

Sternberg, R.W., Cacchione, D.A., Drake, D.E., Kranck, K., 1986. Suspended sediment transport in an estuarine tidal channel within San Francisco Bay, California. Marine Geology 71, 237–258.

U.S. Geological Survey (USGS), 2011. Water-resources data for the United States, Water Year 2010: U.S. Geological Survey Water-Data Report WDR-US-2010, site 11460000.

Uncles, R.J., Stephens, J.A., 1993. Nature of the turbidity maximum in the Tamar Estuary, U.K. Estuarine, Coastal and Shelf Science 36, 413–431.

Uncles, R.J., Stephens, J.A., 2010. Turbidity and sediment transport in a muddy subestuary. Estuarine, Coastal and Shelf Science 87, 213–224.

Warrick, J.A., Milliman, J.D., 2003. Hyperpycnal sediment discharge from semiarid southern California rivers: implications for coastal sediment budgets. Geology 31, 781–784.

Wright, S.A., Schoellhamer, D.H., 2004. Trends in the sediment yield of the Sacramento River, California, 1957–2001. San Francisco Estuary and Watershed Science 2, 14pp.